Adsorbent materials from paper industry waste materials and their use in Cu(II) removal from water

A. Méndez   , S. Barriga , J.M. Fidalgo[a], G. Gascó

Departamento de Ingeniería de Materiales. E.T.S.I.Minas. Universidad Politécnica de Madrid. C/Ríos Rosas, n°. 21, 28003 Madrid,Spain
Departamento de Edafología. E.T.S.I.Agrónomos. Universidad Politécnica de Madrid. Avda Complutense s/n, 28040 Madrid, Spain

ABSTRACT

This paper deals with the removal of Cu^{2+} from water using adsorbent materials prepared from paper industry waste materials (one de-inking paper sludge and other sludge from virgin pulp mill). Experimental results showed that de-inking paper sludge leads to mesoporous materials ($V_{mic}/V_T = 0.13$ and 0.14), whereas the sludge from virgin pulp mill produces high microporous adsorbents ($V_{mic}/V_T = 0.39$ and 0.41). Adsorbent materials were then used for Cu^{2+} removal from water at acid pH. During water treatment, heavy metals lixiviation from adsorbent materials was not produced. However, important Ca and Mg leaching was observed. Final pH significantly increases after treatment of water with adsorbent materials probably due to their elevated $CaCO_3$ content. In general, highest Cu^{2+} removal was obtained using adsorbent materials from de-inking paper sludge. This result could be due to their higher content in oxygenated surface groups, high average pore diameter, elevated superficial charge density, high $CaCO_3$ amount and high Ca and Mg exchange content.

1. Introduction

Paper pulp manufacturing separates cellulose fibres using both, mechanical and chemical process and generates important amount of waste materials. Currently, they are disposed through combustion or landfilling. So, the reuse of these organic wastes in any industrial process is a high priority today.

In recent years, an increasing proportion of recycled fibres are used in paper industries due to their important environmental and economical benefits. A ton of pulp produced from recycled paper requires 60% less energy to manufacture than a ton of bleached virgin kraft pulp   . However, removing the ink, clay, coatings and contaminants from waste paper in order to produce recycled paper creates large amounts of de-inking paper sludge (DPS). In Spain, more than 200,000 t of DPS were produced during 2006

Due to their high organic matter content, DPS could be used as amendment to improve or restore soil fertility and biological functioning   . Used in agriculture and in restoration, DPS amendments increase yield and plant growth and improve soil properties such as: organic matter content, water holding capacity and cation exchange capacity   . So, DPS provide materials serving as a long-term source of organic matter   . However, since DPS are poor in phosphorus and nitrogen, supplemental P or N fertilizers have to be added to improve the growth of woody species

Other possible alternative is composting. Nevertheless, the high C/N of DPS limits their used and some studies are focused on their composting mixed with some organic waste materials such as poultry manure   or wastewater sludge

In recent years, large volume of heavy metals has been disposed on the environment. Due to their toxicity, numerous treatments have been developed for the metal removal from contaminated waters. Conventional methods like precipitation are unfavourable especially when dealing with large volumes of water which contain metal ions in low concentration. Frequently, after precipitation and following filtration, concentration of metal ions still remains on the level of few $mg\,L^{-1}$ and a great amount of waste precipitated was produced. Other methods like ion-exchange or adsorption with commercial activated carbon are expensive and the high cost could limit their use. In the last years, many efforts have been focused on low cost adsorbent materials from pyrolysis of waste materials such as sewage sludges   , agricultural by-products   , biomass residues   or recycled plastics   . DPS and other organic waste materials from paper industry could be interesting precursors of these carbon materials due to their high carbon content and specially, cellulose fibres proportion.

The main objective of this work is to study the use of adsorbent materials obtained from pyrolysis of paper industry waste materials in the Cu^{2+} removal from water.

2. Experimental

2.1. Raw material

Two paper industry waste materials were used as adsorbent precursors: one de-inking paper sludge from recycled paper-press manufacturing (HP) and other organic sludge from eucalyptus virgin pulp mill (RT). Samples were air-dried, crushed and sieved through 2 mm mesh.

2.2. Raw materials characterisation

Both samples were characterised as follows:

pH and electrical conductivity (EC) were measured in a Crison micro-pH 2000 and a Crison 222 conductivimeter, respectively, after stirring a mixture of each sample and distilled water ($4 \, g \, L^{-1}$) for 2 h.

Cation exchange capacity (CEC) was determined with $NH_4OAc/HOAc$ at pH 7.0 by the Sumner and Miller method

Total organic matter (TOM) of both samples was determined by burning samples at $540 \, °C$ during 4 h in a Heron 12-PR/300 furnace.

Ca, Mg, Na, K, Cr, Ni, Cu, Zn, Cd, Pb of samples were extracted with HCl and HNO_3 and determined following the 3051a USEPA method using a PerkinElmer 403 atomic absorption spectrophotometer.

$CaCO_3$ content was measured by treating the sample with HCl and measuring the evolved CO_2 manometrically.

Scanning electron microscopy (SEM) was carried out by means of a Hitachi S-570, Scanning Electron Microscope coupled with an energy dispersive X-ray spectroscopy (EDS), Rontec.

X-ray diffraction (XRD) of raw materials was performed in a Philips PW-1729 diffractometer.

The surface functional groups were investigated by Fourier transform infrared spectrometry (FTIR). The FTIR spectra of samples were obtained with a Broker Vector 22 spectrometer. Transparent pellets were prepared using KBr.

Thermal analysis of samples was performed using a Labsys Setaram equipment. About 20 mg of sample was heated at $10 \, °C \, min^{-1}$ until $900 \, °C$ with a flow nitrogen rate of $40 \, mL \, min^{-1}$.

2.3. Preparation of adsorbent materials

Adsorbent materials were prepared as follows: 20 g of samples were placed in a covered ceramic cup that was introduced in a covered nickel recipient. The cavity between the two recipients was filled up with fuel coke particles (<1 mm). As the temperature increases, O_2 of air is consumed by fuel coke particles and samples were pyrolysed in the inert atmosphere generated. An electrical furnace model Heron 12-PR/300 was used and the temperature was increased to $650 \, °C$ at a rate of $3 \, °C \, min^{-1}$ or $10 \, °C \, min^{-1}$. In both cases, the final temperature was maintained for 2 h. The char yield was calculated by the relation between the weight of samples before and after pyrolysis treatment.

2.4. Adsorbent materials characterisation

Adsorbent materials were characterised as follows:

Scanning electron microscopy (SEM) was carried out by means of a Hitachi S-570, Scanning Electron Microscope coupled with EDS, Rontec.

The characterisation of porosity was made from the data of sorption–desorption of N_2 at 77 K in a Micromeritics ASAP 2010

volumetric system. The mean surface area was evaluated from the BET equation.

pH, CEC and EC of adsorbent materials were determined by the same procedure described in Section 2.2.

The superficial charge density (ρ) was calculated from BET surface area and CEC values, as follows:

$$\rho = 10^{-3} \frac{CEC}{BET}$$

Functional groups of adsorbents were analysed by FTIR in a same way as was described previously (Section 2.2)

Ash content of adsorbents was determined by heating 10 g of sample in an electrical furnace at $540 \, °C$ during 4 h in air atmosphere.

2.5. Metal removal

Adsorbent materials were used in the removal of Cu^{2+} from water. To evaluate metal adsorption, 20 mL of Cu^{2+} solution were mixed with 50 mg of adsorbent and stirred during 2 h at 300 rpm. Then, solutions were filtrated to separate the suspension of carbon particles and the metal final concentration was evaluated by atomic absorption using a by PerkinElmer 403 atomic absorption spectrophotometer. pH of solutions was adjusted to pH 5 to avoid metal precipitation. Ca, Mg, Na, K, Cr, Ni, Cu, Zn, Cd, Pb of solutions after Cu^{2+} removal were evaluated using the same PerkinElmer 403 atomic absorption spectrophotometer. A commercial activated carbon, CAC, supplied by Panreac S.A was used in order to compare experimental results.

3. Results and discussion

3.1. Raw material characterisation

Table 1 summarises main properties of paper industry waste materials used in this work. HP and RT show similar pH and EC values. Both were lightly basic with low EC values. Main differences between both materials were found in the TOM, CEC and $CaCO_3$ content. CEC and $CaCO_3$ content of HP were significantly elevated ($25.37 \, cmol_{(c)} \, kg^{-1}$ and 24.4 wt%, respectively) while RT shows higher organic matter content (88.7 wt%). During de-inking process of paper-press, removal of inorganic additives of paper, principally $CaCO_3$ and clays, was produced leading to waste materials with high inorganic matter content than waste products obtained from virgin pulp mill. These results were according with the elevated Ca content of HP (Table 2). In general, HP shows higher metal concentration than RT (except of Cd). This could be related to the presence of inks and clays removed during recycling process of paper wastes. In general, these values were higher than that obtained by other authors [19] but in both cases, they were lower than Spanish Legislation limits for their possible agricultural application

Fig. 1 shows representative SEM micrographs of two paper industry waste materials. It could be observed as HP was composed by irregular cracked and short cellulose fibres in a mixture with aggregates of mineral particles (Fig. 1a and b). EDX analyses prove that they are composed from Ca, Al and Si. These results were according to previous works that showed as mineral matter of

Table 1
Main properties of paper industry waste materials.

Waste material	CEC ($cmol_{(c)} \, kg^{-1}$)	pH	EC ($\mu S \, cm^{-1}$)	TOM (%)	$CaCO_3$ (%)
HP	25.37	7.77	88	35.0	24.4
RT	19.10	7.72	75	88.7	6.1

Waste material	Concentration (mg kg^{-1})								
	Ca	Mg	Na	K	Cu	Ni	Cd	Zn	Pb
HP	65969	288	1252	32	367	170	9.8	1918	57
RT	12813	266	1404	20	*	2.1	24.8	*	*

* Below detection limit.

de-inking paper sludges were formed mainly by clays and calcium carbonate

SEM micrographs of RT show that this paper waste was composed by agglomerates of uniform fibres with an average diameter of about 10–20 μm. In this case, the analysis by EDX shows the presence of small quantities of Ca.

The mineralogy of raw samples was studied by XRD (Fig. 2). It could be observed as the mineral fraction of HP (Fig. 2(a)) is pre-dominantly composed by calcite (c) and kaolinite (k), whereas RT (Fig. 2(b)) shows an elevated content of cellulose fibres (cel) with calcite (c) and quartz (q).

Fig. 3 shows FTIR of HP and RT samples. Main differences between both samples are due to the presence of more bands in HP spectrum as typical kaolinite bands at 3693 and 3619 cm^{-1} and characteristic bands of CaCO$_3$ at 1426 and 875 cm^{-1}. Other differences were related with the organic matter composition,
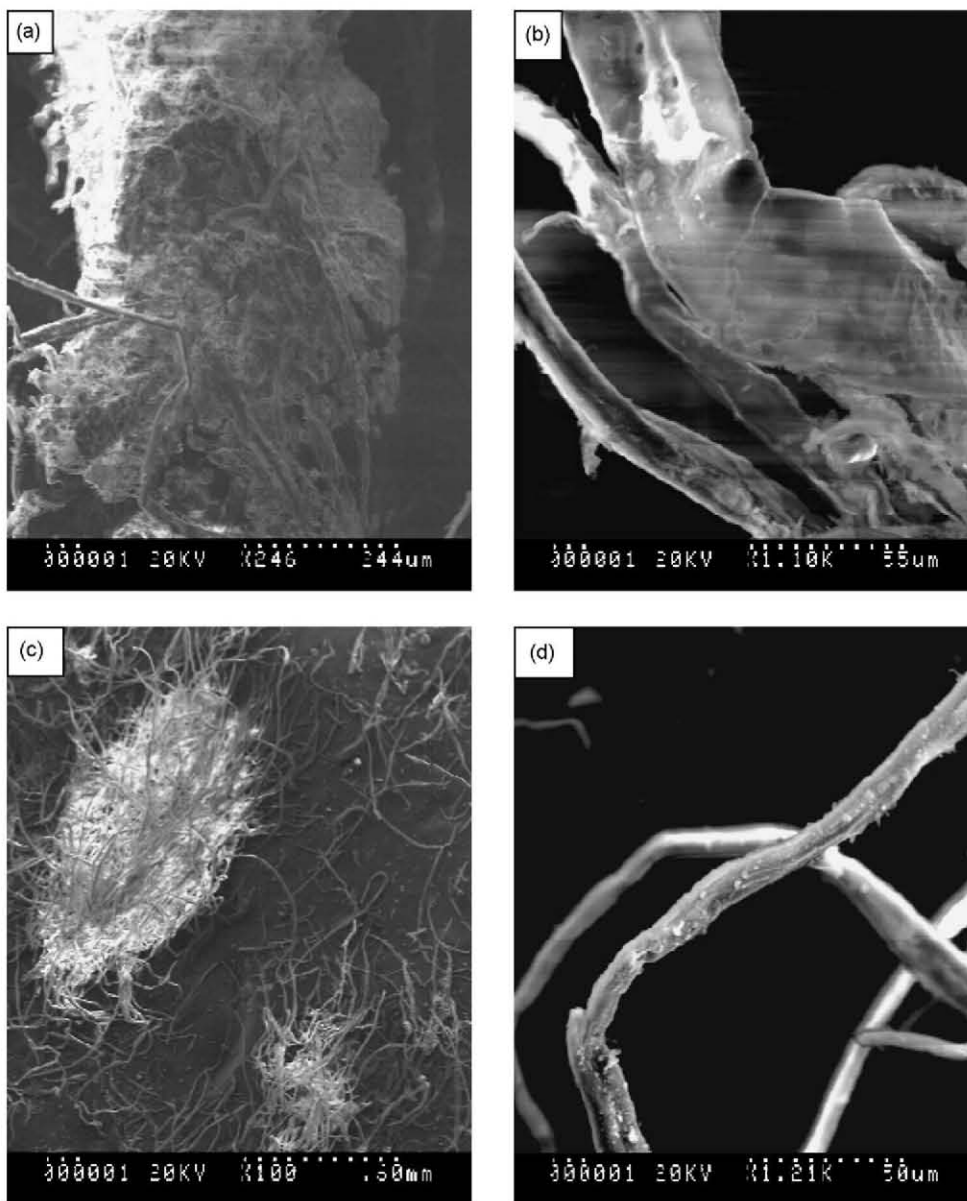

Fig. 1. Representative SEM micrographs of paper industry waste materials (a) and (b) HP; (c) and (d) RT.
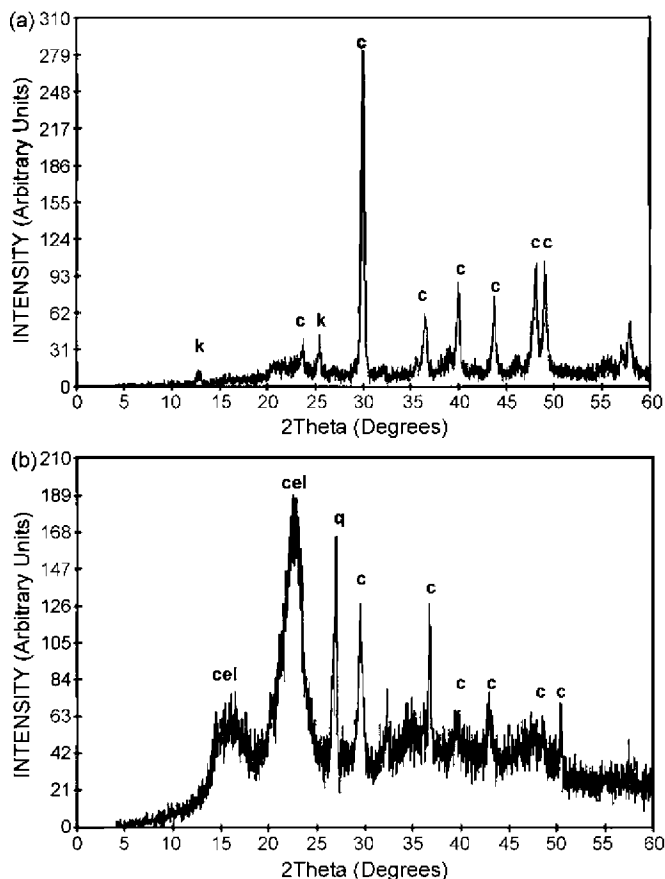
Fig. 2. XRD patterns of raw samples: calcite (c); kaolinite (k); cellulose fibres (cel), quartz (q).

mainly cellulose fibres   In both cases, typical bands of cellulose were present: between 3500 and 3000 cm^{-1} it could be observed the characteristic broad band of OH stretching vibration; bands at 2916 and 2849 cm^{-1} correspond to alkyl groups whereas O–H deformation vibration appear at 1627 cm^{-1}. The two small bands corresponding to deformation modes of C–H and C–OH of cellulose are observed in the FTIR spectra of RT at 1370 and 1315 cm^{-1}, respectively. In the HP, probably they are included in the broad band of carbonates. The bands at 1163 and 1090 cm^{-1} could be related to the presence of C–O–C bonds. Finally, in the FTIR spectrum of HP two new bands at 1724 and 1794 cm^{-1}, typical of C=O bond could be observed, probably due to the oxidation of cellulose fibres or the presence of organic compounds with oxygenated groups.
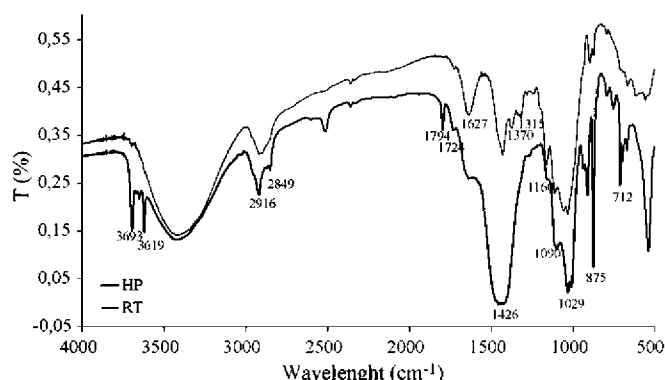

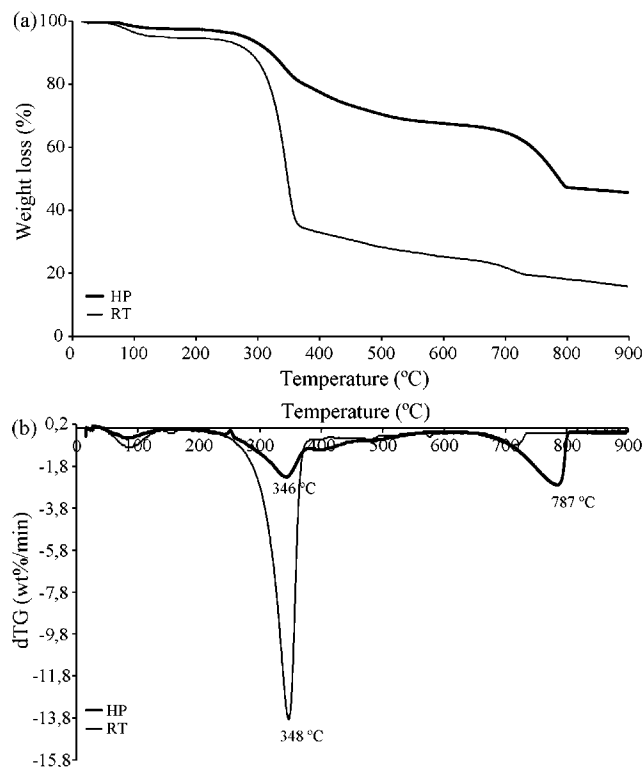**Fig. 3.** FTIR spectra of raw samples.

Fig. 4. TG and dTG of raw samples.

Fig. 4 shows TG (Fig. 4(a)) and dTG (Fig. 4(b)) of HP and RT samples. Main differences between both samples were due to their different composition. In both cases, four areas could be distinguished: First, at $T < 150\,°C$ the weight loss is originated by the moisture release of samples. At temperatures, between 250 and 380 °C, decomposition of cellulose fibres was produced. From 400 to 650 °C, weight loss observed in HP sample could be attributed to the kaolinite dehydration and pyrolysis reactions of other organic compounds present in de-inking paper sludge. Finally, at temperatures higher than 650 °C, decomposition of carbonates was produced.

3.2. Pyrolysis of paper industry wastes

Pyrolysis of paper industrial waste materials was performed at 650 °C. From Fig. 4 it could be observed that at this temperature pyrolysis of cellulose and dehydration of clays was finished, whereas carbonates decomposition starts at higher temperatures. Table 3 shows char yield after pyrolisis at 650 °C. HP leads to higher yields than RT as a result of their high inorganic matter content (Table 1). In general, char yield decreases when the heating rate increases from 3 to 10 °C min^{-1}, according to Khezami et al.

3.3. Adsorbent materials

Table 4 shows main adsorbents properties. All materials show a basic pH, especially for HP-3, HP-10 and CAC (pH $\geq$ 10). The

Table 3
Pyrolysis yields of paper industrial waste materials.

Waste material	Heating rate ($C\,min^{-1}$)	Adsorbent	Char yield (wt%)
HP	3	HP-3	60.8
HP	10	HP-10	59.0
RT	3	RT-3	27.8
RT	10	RT-10	25.4

Table 4
Adsorbent materials properties.

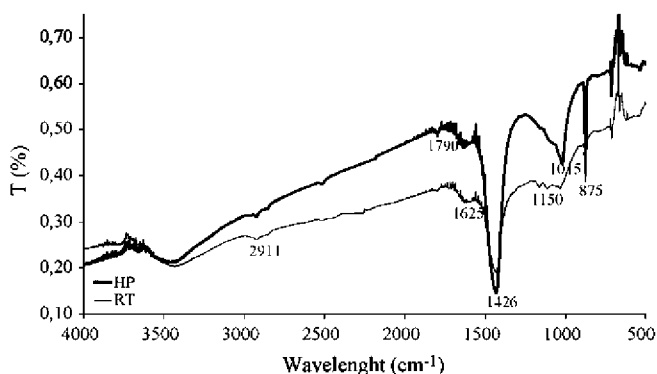| Adsorbent material	CEC (cmol$_{(c)}$ kg^{-1})	pH	EC (μS cm^{-1}) (25 °C)	Ash content (wt%)
HP-3	11.3	10.3	126.1	81.8
HP-10	14.2	10.2	161.2	83.1
RT-3	20.4	9.2	110.6	43.7
RT-10	20.2	9.1	102.3	47.6
CAC	11.4	10.0	67.5	1.5

Fig. 5. FTIR spectra of adsorbent materials HP-3 and RT-3.

pH increases after thermal treatment as a result of polymerization/condensation reactions and acidic surface groups releases during pyrolysis   So, the carbonate enrichment after pyrolysis of samples contributed to the pH increase. Comparison of Tables 1 and 4 shows as electrical conductivity augments with thermal treatment as a result of inorganic matter concentration after pyrolysis treatment of wastes. Cation exchange capacity of adsorbents obtained by pyrolysis of organic sludge from virgin pulp mill (RT-3 and RT-10) was higher than in case of HP-3, HP-10 and CAC.

FTIR of adsorbents HP-3 and RT-3 are showed in Fig. 5. After pyrolysis, main functional oxygenated and alquil groups of cellulose disappear. Main bands at 1426 and 875 cm^{-1} correspond to carbonates. Differences between HP-3 and RT-3 were due to the presence in HP-3 of more intense absorption at 1790 cm^{-1} (C=O bond) and 1015 cm^{-1} (C—OH or C—O—C bonds).

Fig. 6 shows representative SEM micrographs of adsorbents prepared from HP and RT waste materials. Not important differences were found between materials heat treated at 3 or 10 °C min^{-1}. SEM photographs enable to see the shape of the fibres. Adsorbents obtained from HP show short and irregular cellulose carbon fibres and inorganic particles, in a similar way than original de-inking paper sludge (Fig. 1a and b). Recycled process of waste paper and subsequent pyrolysis treatment leads to damage of fibres. Adsorbents obtained from RT show more homogeneous structures (Fig. 6c and d). However, their comparison with original organic sludge (Fig. 1c and d) show that cellulose carbon fibres are shorter (Fig. 6c) as a result of thermal treatment. In this case, cellulose carbon fibres were less damaged (Fig. 6d) than in adsorbents from de-inking paper sludge (Fig. 6a and b).

Table 5 shows BET surface area, micropore and mesopore volume of four adsorbent materials prepared from HP and RT. In general, low porosity values were obtained. Highest BET surface areas corresponds to RT-3 and RT-10 adsorbents (274.74 and 245.47 m^2 g^{-1}, respectively), whereas lowest values were observed in HP-10 and HP-3 samples (75.05 and 88.40 m^2 g^{-1}, respectively). This result was related with the elevated proportion of fibres of RT-3 and RT-10, whereas HP leads to materials with high ash content (Table 4). Other important difference was related with V_{mic}/V_T of four samples. De-inking paper sludge leads to adsorbent materials with high mesoporous content as was reflected by their low V_{mic}/V_T value (0.13 and 0.14). However, organic sludge from eucalyptus pulp mill leads to microporous adsorbents, with V_{mic}/V_T of 0.41 and 0.39.

Generally, the BET surface area increases when the heating rate decreases from 10 to 3 °C min^{-1}, probably due to larger residence time of samples inside the pyrolysis reactor. So, the micropore volume and V_{mic}/V_T increases when the heating rate decreases, contrary to experimental results obtained by other authors

Finally, the superficial charge density (ρ) of four adsorbents was calculated from corresponding BET surface areas and CEC values. This parameter could be related with the ability of adsorbent materials to interact with metal ions. Table 5 shows that high values correspond to HP-3 and HP-10 as a result of their lowest BET areas.

3.4. Cu^{2+} removal

Table 6 shows Cu^{2+} removal by adsorbent materials and using standard solutions of 50 mg Cu^{2+} L^{-1} at pH 5. Highest Cu^{2+} removal was produced with HP-3 and HP-10 with final Cu^{2+} concentration <0.002. It could be observed that in spite of the low porosity, adsorbents from paper industry waste materials were competitive to activated carbons in Cu^{2+} removal. Heavy metals and salts content after water treatment were measured in order to study their possible lixiviation from adsorbent materials (Table 6). It was interesting to note that not heavy metal leaching was produced during treatment of water. However, relatively elevated concentrations of Ca^{2+} and Mg^{2+} were detected after treatment of Cu^{2+} solutions with adsorbents. Also, in case of RT-3 and RT-10, important Na$^+$ and K$^+$ release was produced. These results were in accordance with that obtained previously   . It can be seen from Tables 5 and 6 that the adsorption capacities of the different adsorbent materials were not in accordance with their surface area   Previous works have showed that the high removal ability of materials obtained from sewage sludge pyrolysis at 650 °C could be attributed to cation exchange reactions between calcium and magnesium in aluminosilicates (formed on their surface during heat treatment) and

Table 5
BET surface area, micropore and mesopore volume of adsorbents.

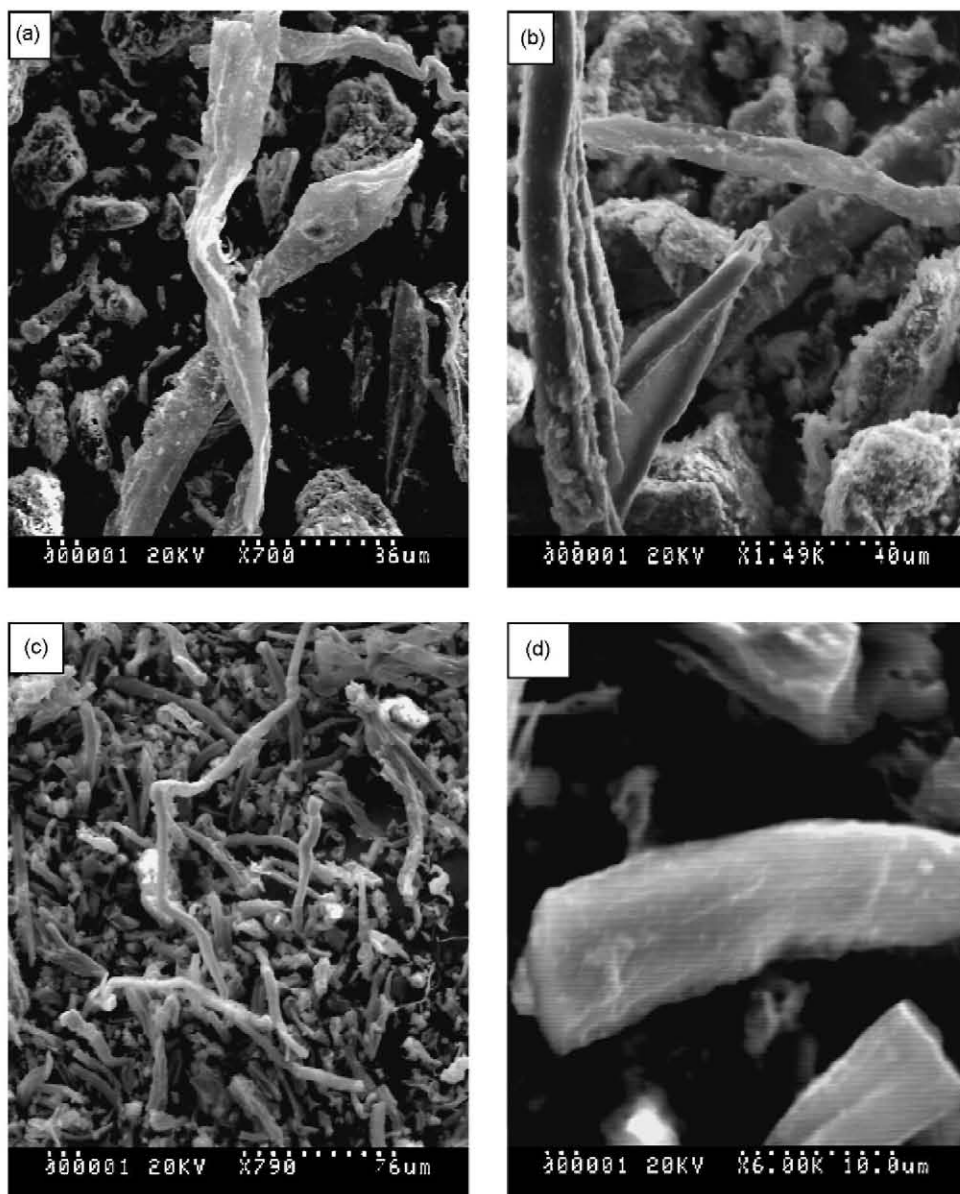| Adsorbent material	BET (m^2 g^{-1})	Micropore area (m^2 g^{-1})	Mesopore area (m^2 g^{-1})	V micropore (cm^3 g^{-1})	V_{mic}/V_T	Average pore diameter (nm)	ρ (cmol$_{(c)}$ m^{-2})
HP-3	88.40	42.51	45.89	0.014205	0.14	4.5303	1.28 × 10^{-4}
HP-10	75.04	38.38	36.66	0.013193	0.13	5.4453	1.89 × 10^{-4}
RT-3	274.74	166.61	108.13	0.061020	0.41	2.1597	7.42 × 10^{-5}
RT-10	245.47	149.65	95.82	0.054881	0.39	2.2659	8.22 × 10^{-5}

Fig. 6. Representative SEM micrographs of adsorbents: (a) and (b) from HP; (c) and (d) from RT.

Table 6
Final metal concentration of Cu^{2+} solution (50 mg L^{-1} at pH 5) after treatment with adsorbents.

Adsorbent material	Final metal concentration (mg L^{-1})									
	Cu	Pb	Cd	Zn	Cr	Ni	Ca	Mg	Na	K
HP-3	<0.002	<0.01	<0.001	<0.001	<0.003	<0.005	34.5	5.8	0.6	0.7
HP-10	<0.002	<0.01	<0.001	<0.001	<0.003	<0.005	32.4	5.5	1.2	1.0
RT-3	5.3	<0.01	<0.001	<0.001	<0.003	<0.005	25.3	2.5	5.7	2.0
RT-10	7.1	<0.01	<0.001	<0.001	<0.003	<0.005	22.8	3.3	6.8	1.9
CAC	27.7	<0.01	<0.001	<0.001	<0.003	<0.005	8.9	6.4	0.3	9.0

Table 7
Final metal concentration of acid solution at pH 5 after treatment with adsorbents.

Adsorbent material	Final metal concentration (mg L^{-1})									
	Cu	Pb	Cd	Zn	Cr	Ni	Ca	Mg	Na	K
HP-3	<0.002	<0.01	<0.001	<0.001	<0.003	<0.005	16.6	4.3	0.6	0.4
HP-10	<0.002	<0.01	<0.001	<0.001	<0.003	<0.005	16.2	4.5	1.2	0.6
RT-3	<0.002	<0.01	<0.001	<0.001	<0.003	<0.005	13.4	2.3	5.1	1.3
RT-10	<0.002	<0.01	<0.001	<0.001	<0.003	<0.005	13.4	3.2	6.8	1.3

Table 8
pH of Cu^{2+} solutions before and after treatment with adsorbents.

Adsorbent material	Initial pH	Final pH
HP-3		7.2
HP-10		6.7
RT-3	5.0	6.3
RT-10		6.1
CAC		5.6

copper   In this way, Table 7 shows heavy metals and salts content after adsorbent materials treatment with acid solution at pH 5 without Cu^{2+} addition. It is interesting to note that less Ca^{2+} and Mg^{2+} was produced after treatment of acid solutions without Cu^{2+} that more cation exchange reactions were produced in the presence of Cu^{2+}. However, similar Na^+ and K^+ concentrations were observed in the presence or absence of Cu^{2+} (Tables 6 and 7, respectively).

Other works carried out by Phan et al. [27] have showed that raw fibres with low surface area were more efficient than carbonized or physically activated fibres for Cu^{2+} removal may be due to the great influence of carboxylic surface groups on the removal of metal cations indicating by ion-exchange reactions. FTIR analysis have shown that more oxygenated groups were present in adsorbent materials from de-inking paper sludge, HP-3 and HP-10, and probably contributed to their high Cu^{2+} removal capacity.

Finally, Table 8 shows the final pH of solutions after treatment with adsorbent materials. pH significantly increases after removal of Cu^{2+} in accordance with results showed by Lu et al. [28] in the removal of Zn from aqueous solutions using crab carapace biosorbent. At low pH, $CaCO_3$ dissolved as Ca^{2+} and CO_3^{2-} and then, CO_3^{2-} reacted with proton to form HCO_3^- and H_2CO_3. So, the CO_3^{2-} hydrolysis reactions produce the pH increases observed in Table 8, especially with RT-3 and RT-10 adsorbents due to their elevated carbonate content. At this pH important precipitation of copper hydroxide or hydroxicarbonates could be produced.

Therefore, the removal mechanism for heavy metals seems to be related with the following factors:

- Chemical reactions between the acidic sites of adsorbents and heavy metals, especially cation exchange reactions.
- Specific surface area and high volume of mesopores.
- Precipitations of metal hydroxides or hydroxicarbonates due to the pH increases of solutions after their mixture with adsorbents.

Due to high removal of adsorbent materials from de-inking paper sludges, HP-3 was selected for subsequent experiments at pH 3 and pH 5 with Cu^{2+} concentration from 10 to 200 mg L^{-1}. Table 9 shows removal of Cu^{2+} and final pH after treatment of different Cu^{2+} solutions with HP-3 adsorbent. In both cases, treatment of solutions at pH 3 and pH 5 with HP-3 leads to similar final pH $\geq$ 6. So, Cu^{2+} precipitation as $Cu(OH)_2$ would be similar in both cases. However, highest Cu^{2+} removal were obtained after treatment of solutions with initial pH 5, indicating that other mechanism as

Table 9
Removal of Cu^{2+} and final pH after treatment of different Cu^{2+} solutions with HP-3 adsorbent.

Initial Cu^{2+} concentration (mg L^{-1})	Initial pH 3		Initial pH 5	
	Removal (wt%)	Final pH	Removal (wt%)	Final pH
10	98.3	7.4	100.0	7.5
25	83.8	7.0	100.0	7.3
50	46.9	6.5	100.0	6.4
100	23.3	5.9	45.7	6.2
150	18.0	6.0	30.3	6.0
200	12.1	5.9	27.1	5.9

cation exchange reactions take place. As pH increases, more surface functional groups dissociate to provide metal binding sites which results in higher Cu^{2+} adsorption.

4. Conclusions

1. Waste materials from paper industry seem to be adequate adsorbent materials precursors. De-inking paper sludge leads to interesting mesoporous materials, whereas organic sludge from eucalyptus pulp mill produces high microporous adsorbents.
2. During water treatment with adsorbent materials obtained from paper industry waste materials, lixiviation of metals was not observed. However, important Ca^{2+} and Mg^{2+} leaching were produced as a result of cation exchange reactions.
3. pH significantly increases after treatment of acid water with adsorbent materials due to their elevated $CaCO_3$ content and Cu^{2+} precipitation could be produced.
4. Cu^{2+} removal was higher for adsorbents obtained from de-inking paper sludge. The elevated oxygenated surface groups, high average pore diameter, elevated superficial charge density and Ca and Mg exchange content of adsorbents from de-inking paper sludges could be responsible of their higher Cu^{2+} removal capacity.

Acknowledgements

References

C.G. Thompson, Recycled Papers. The Essential Guide, MIT Press, Cambridge, 1992.

Diagnóstico de la generación y gestión de residuos sólidos en la industria papelera española. ASPAPEL, Madrid, 2007.

M.H. Chantigny, D.A. Angers, C.J. Beauchamp, Aggregation and organic matter decomposition in soils amended with de-inking paper sludge, Soil Science Society of America Journal 63 (1999) 1214–1221.

A. Fierro, D.A. Angers, C.J. Beauchamp, Decomposition of paper de-inking sludge in a sandpit minesoil during revegetation, Soil Biology and Biochemistry 32 (2000) 143–150.

M.H. Chantigny, D.A. Angers, C.J. Beauchamp, Active carbon pools and enzyme activities in soils amended with de-inking paper sludge, Canadian Journal of Soil Science 80 (2000) 99–105.

P. Filiatrault, C. Camiré, J.P. Norrie, C.J. Beauchamp, Effects of de-inking paper sludge on growth and nutritional status of alder and aspen, Resources, Conservation and Recycling 48 (2006) 209–226.

M.H. Charest, C.J. Beauchamp, Composting of de-inking paper sludge with poultry manure at three nitrogen levels using mechanical turning: behaviour of physico-chemical parameters, Bioresource Technology 81 (2002) 7–17.

T. Gea, A. Artola, A. Sánchez, Composting of de-inking sludge from the recycled paper manufacturing industry, Bioresource Technology 96 (2005) 1161–1167.

A. Méndez, G. Gascó, M.M.A. Freitas, G. Siebielec, T. Stuczynski, J.L. Figueiredo, Preparation of carbon-based adsorbents from pyrolysis and air activation of sewage sludges, Chemical Engineering Journal 108 (2005) 169–177.

A. Ros, M.A. Lillo-Ródenas, E. Fuente, M.A. Montes-Morán, M.J. Martín, A. Linares-Solano, High surface area materials prepared from sewage sludge-based precursors, Chemosphere 65 (2006) 132–140.

M. Madhava Rao, G.P. Chandra Rao, K. Seshaiah, N.V. Choudary, M.C. Wang, Activated carbon from Ceiba pentandra hulls, an agricultural waste, as an adsorbent in the removal of lead and zinc from aqueous solutions, Waste Management 28 (2008) 849–858.

M.T. González, F. Rodríguez-Reinoso, A.N. García, A. Marcilla, CO_2 activation of olive stones carbonized under different experimental conditions, Carbon 35 (1997) 159–165.

S.S. Baral, S.N. Das, G.R. Chaudhury, Y.V. Swamy, P. Rath, Absorption of Cr(VI) using thermally activated weed Salvinia cucullata, Chemical Engineering Journal 139 (2008) 245–255.

O. Gerçel, H.F. Gerçel, Adsorption of lead(II) ions from aqueous solutions by activated carbon prepared from biomass plant material of Euphorbia rigida, Chemical Engineering Journal 132 (2007) 289–297.

C.O. Ania, J.B. Parra, A. Arenillas, F. Rubiera, T.J. Bandosz, J.B. Pis, On the mechanism of reactive adsorption of dibenzothiophene on organic waste derived carbons, Applied Surface Science 253 (2007) 5899–5903.

M.E. Sumner, W.P. Miller, in: M. Bigham (Ed.), Methods of Soil Analysis. Part 3. Chemical Methods, SSSA, Madison, 1996, pp. 1201–1229.

D.W. Nelson, L.E. Sommers, Total carbon, organic carbon and organic matter, in: J.M. Bigham (Ed.), Methods of Soil Analysis. Part 3. Chemical Methods, SSSA, Madison, 1996, pp. 961–1010.

USEPA, Method 3051a: Microwave Assisted Acid Dissolution of Sediments, Sludges, Soils, and Oils, U.S. Government Printing Office, Washington, 1997.

C.J. Beauchamp, M.-H. Charest, A. Gosselin, Examination of environmental quality of raw and composting de-inking paper sludge, Chemosphere 46 (2002) 887–895.

MAPA-España. Real Decreto 1310/1990, de 29 de octubre, por el que se regula la utilización de los lodos de depuración en el sector agrario. Ministerio de Agricultura, Pesca y Alimentación MAPA de España. Boletín Oficial del Estado 262, 1990, pp. 32339–32340.

R. Vigil de la Villa, M. Frías, M.I. Rojas, I. Vegas, R. García, Mineralogical and morphological changes of calcined paper sludge at different temperatures and retention in furnace, Applied Clay Science 36 (2007) 279–286.

M.C. Silvam, O.R. Lopes, J.L. Colodette, A.O. Porto, J. Rieumont, D. Chaussy, M.N. Belgacem, G.C. Silva, Characterisation of three non-product materials from a bleached eucalyptus kraft pulp mill, in view of valorising them as a source of cellulose fibres, Industrial Crops and Products 27 (2008) 288–295.

L. Khezami, A. Chetouani, B. Taouk, R. Capart, Production and characterisation of activated carbon from wood components in power: cellulose, lignin, xylan, Powder Technology 157 (2005) 48–56.

G. Gascó, C.G. Blanco, F. Guerrero, A. Méndez, The influence of organic matter on sewage sludge pyrolysis, Journal of Analytical and Applied Pyrolysis 74 (2005) 413–420.

F.S. Zhang, H. Itoh, Adsorbents made from waste ashes and post-consumer PET and their potential utilization in wastewater treatment, Journal of Hazardous Materials 101 (2003) 323–337.

M. Seredych, T.J. Bandosz, Removal of copper on composite sewage sludge/industrial sludge-based adsorbents: the role of surface chemistry, Journal of Colloid and Interface Science 302 (2006) 379–388.

N.H. Phan, S. Rio, C. Faur, L. Le Coq, P. Le Cloirec, T.H. Nguyen, Production of fibrous activated carbons from natural cellulose (jute, coconut) fibers for water treatment applications, Carbon 44 (2006) 2569–2577.

S. Lu, S.W. Gibb, E. Cochrane, Effective removal of zinc ions from aqueous solutions using crab carapace biosorbent, Journal of Hazardous Materials 149 (2007) 208–217.